Spatial dependence of gain nonlinearities in InGaAs semiconductor optical amplifier

Gomez-Iglesias, A ; Fenn, J G ; Mazilu, M ; Miller, Alan

Published in:
Applied Physics Letters

DOI:
10.1063/1.2053357

Publication date:
2005

Spatial dependence of gain nonlinearities in InGaAs semiconductor optical amplifier

Alvaro Gomez-Iglesias, Julia G. Fenn, Michael Mazilu, and Alan Miller

Citation: Appl. Phys. Lett. **87**, 121108 (2005); doi: 10.1063/1.2053357
View online: http://dx.doi.org/10.1063/1.2053357
View Table of Contents: http://apl.aip.org/resource/1/APPLAB/v87/i12
Published by the American Institute of Physics.

Spatial dependence of gain nonlinearities in InGaAs semiconductor optical amplifier

Alvaro Gomez-Iglesias, Julia G. Fenn, Michael Mazilu, and Alan Miller
Ultrafast Photonics Collaboration, School of Physics and Astronomy, University of St. Andrews, Fife, KY16 9SS, United Kingdom

(Received 15 April 2005; accepted 29 July 2005; published online 14 September 2005)

Counter-propagating sub-picosecond pulses are used to monitor gain saturation along the waveguide of an InGaAs superlattice semiconductor optical amplifier at 1550 nm wavelength. The functional form of the spatial dependence of gain saturation is found to depend on pulse energy. These observations are interpreted by combining the optical nonlinearities associated with interband carrier dynamics and carrier heating together and their respective time constants. We show that the results are consistent with the predictions of a propagation model. Implications for all-optical switching, particularly in the limit of full saturation across the whole amplifier, are discussed.
 [DOI: 10.1063/1.2053357]

During the last decade, semiconductor optical amplifiers (SOA) have become promising candidates for all-optical processing and switching applications. Interferometric switches exploiting the large SOA resonant optical nonlinearities, such as the Terahertz Optical Asymmetric Demultiplexer (TOAD),[1] have been shown to operate at rates faster than the interband recovery time of the material.[2] For configurations with counter-propagating control and data pulses, the finite device length is a major limitation.[3] However, the spatial dependence of the gain depletion induced by the control pulse across the device is usually overlooked. We report pump-probe experiments with counter-propagating geometry to analyze the role of the gain depletion along the SOA waveguide, and the subsequent refractive index change, in switching operation. A phenomenological rate-equation model was developed to clarify the device behavior.

The study focused on a 1 mm long SOA with AR-coated, angled-facets. It comprises 10 wells and 11 barriers of InGaAs on an InP substrate with peak gain at a wavelength around 1565 nm. The device was characterized by measurements of gain bandwidth, gain saturation, and gain recovery on sub-picosecond timescales, as a function of electrical bias, optical power, and wavelength.

Typical copropagating pump-probe results show a sharp decrease in gain around zero delay attributed to two photon absorption and rapid partial gain recovery, associated with carrier cooling ($\sim$1 ps).[4] The full gain recovery due to the slower interband processes takes hundreds of picoseconds. This is illustrated in Fig. 1, where Δ_N and Δ_T are the initial changes in probe transmission attributed to carrier density depletion and carrier heating, respectively.

The counter-propagating pump-probe experiments reported here employed 700 fs pulses generated by an optical parametric oscillator (OPO), wavelength tunable in the 1500 nm region. As seen in the upper inset of Fig. 2(a), pump (TM polarized) and probe (TE polarized) pulses propagate along the SOA in opposite directions. The results shown in Fig. 2(a), obtained at 70 mA electrical bias and 1555 nm wavelength, differ substantially from those of typical copropagating geometries. On the timescales considered, the slow interband dynamics appear as a negative step change in probe transmission. We observe a gradual gain depletion over 25 ps and only a "tail" of the fast carrier heating recovery.

To understand the slow pace of gain depletion, consider that for a delay $\tau=0$, the probe meets the pump at facet "A" ($x=0$). In this case the probe has propagated through the whole device before the pump has entered the facet and, therefore, no change in transmission is observed. As the probe delay is increased, the crossing point moves within the SOA and, consequently, the probe travels through a progressively longer gain depleted portion of the amplifier. When the delay has been increased to $\tau=2T(\approx 25$ ps), where T is the transit time across the device, the two pulses meet at facet "B" ($x=-L$). It is then, in all cases [see Fig. 2(a)] that the measured gain depletion is largest. The transmission as a function of probe delay shows a distinctly different characteristic depending on the pump pulse energy. At the lowest pump energy shown (curve I), the gradient of the trace becomes more negative with increasing probe delay. However, the curves measured at higher input energies (II and III) are steeper for small delays and their slope decreases as a function of probe delay.

To explore our results, we use a model based on phenomenological rate equations. The SOA is split into thin slices and the temporal carrier dynamics induced by the incoming pump are solved for every slice. The subsequent time dependent change in gain is then used to simulate iteratively

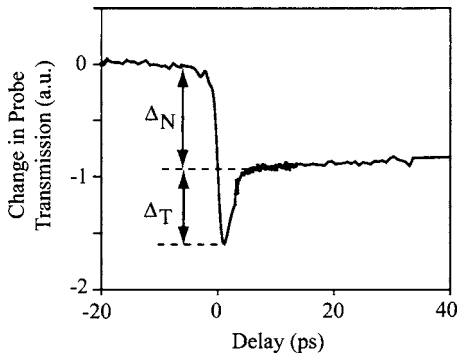

FIG. 1. Example of a typical co-propagating pump-probe trace. Δ_N and Δ_T are the initial changes in probe transmission due to carrier density depletion and carrier heating, respectively.

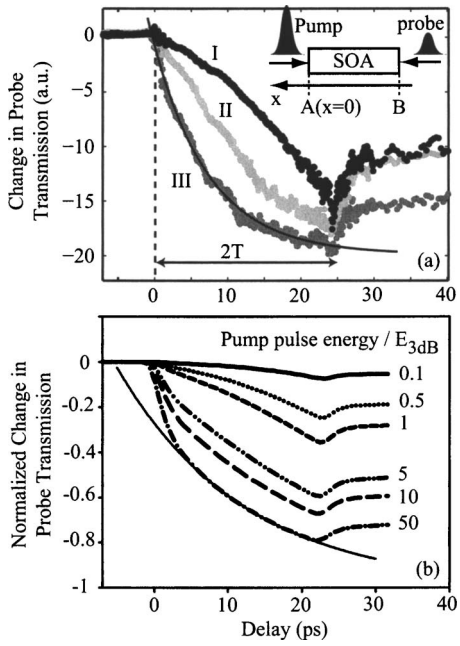

FIG. 2. (a) Counter-propagating pump-probe traces measured at 70 mA bias for input pulses at 1555 nm wavelength, with energies of 70(I), 170(II), and 700(III) fJ. (b) Calculated counter-propagating pump-probe traces for a range of different pump pulse energies using the model. $E_{3\ \mathrm{dB}}$ corresponds to the input pulse energy for which the device gain drops 3 dB with respect to its small-signal value. The solid black thin lines in (a) and (b) show the fittings using Eq. (4).

the probe propagation through consecutive slices. The total gain in the SOA may be defined as $g=g_N+g_T$, where g_N is the carrier density dependent gain and g_T is the decrease in gain due to carrier heating.[5–7]

The gain temporal dynamics can be expressed as

$$\frac{\partial g_N}{\partial t}=\frac{g_0-g_N}{\tau_N}-g\frac{P}{E_{\mathrm{sat}N}}, \tag{1}$$

$$\frac{\partial g_T}{\partial t}=-\frac{g_T}{\tau_T}-g\frac{P}{E_{\mathrm{sat}T}}, \tag{2}$$

where P is the optical power of the propagating pulse and g_0 is the small-signal gain. $E_{\mathrm{sat}N}$ and $E_{\mathrm{sat}T}$ are the saturation energies associated with carrier density changes and carrier heating respectively, as defined in the literature.[6] τ_T is the fast time constant with which carriers cool to the lattice temperature via scattering with phonons and τ_N is the slow recovery associated with interband transitions.

The power of the pump through a small slice of the SOA of thickness Δl, is calculated as

$$P_{\mathrm{out}}(t)\approx P_{\mathrm{in}}(t)\exp\{[\Gamma g(z_i,t)-\alpha_{\mathrm{int}}]\Delta l\}, \tag{3}$$

where $g(z_i,t)$ is the gain at position z_i (ith slice) at time t. The input pulses have a Gaussian intensity profile of width τ_p. Γ is the confinement factor and α_{int} accounts for the internal losses. The probe pulse energy is chosen to be small so that it does not modify the carrier population significantly.

Figure 2(b) shows normalized traces for different pump pulse energies. The model parameters were chosen within the typical ranges found in the literature, namely, $\Gamma=0.3$, $E_{\mathrm{sat}N}=2$ pJ, and $E_{\mathrm{sat}T}=0.5$ pJ. On the other hand, the small-signal gain $g_0=130\ \mathrm{cm}^{-1}$ and the recovery times $\tau_N=251$ ps and $\tau_T=1.2$ ps were obtained from independent experiments made on this amplifier.

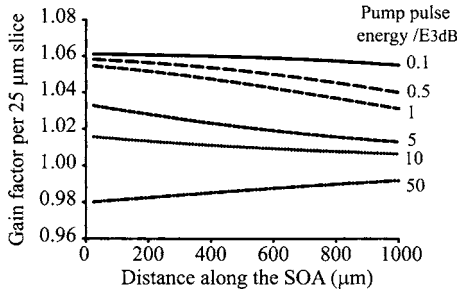

FIG. 3. Gain per slice as the pump propagates along the length of the SOA, calculated for the same range of input pulse energies (in units of $E_{3\ \mathrm{dB}}$) as in Fig. 2(b).

As observed in Fig. 2(b), increasing the pump energy accelerates the gain depletion, consistently with the experimental results. $E_{3\ \mathrm{dB}}$ is the input pulse energy for which the device gain is half of its small-signal value and is dictated mostly by $E_{\mathrm{sat}N}$, $E_{\mathrm{sat}T}$, the recovery times τ_N and τ_T, and the device length.

Figure 3 shows the gain available per slice as a function of position for different pump pulse energies, calculated in our model as the ratio between the output and input pulse energies in a given slice. The pump is amplified as it propagates along the device and, as a result, gain depletion increases. However, it is only at the highest input energies shown that the amplification of the pump is sufficient to saturate the gain in a portion of the device. Furthermore, a high energy pulse can heavily saturate the gain along the whole length of the device, as shown by the $50E_{3\ \mathrm{dB}}$ curve in Fig. 3 (The gain is smaller than unity due to the internal loss, taken to be $\alpha_{\mathrm{int}}=15\ \mathrm{cm}^{-1}$.) Under these conditions, for a delay τ, the probe meets the pump at $x=-\tau L/2T$ and travels first through a small portion of the SOA of length L_T (dictated by τ_T) where the gain depletion is due both to changes in carrier density and carrier heating. However, in the rest of the waveguide, carriers had time to cool so the probe experiences an uniform gain due to carrier density depletion alone. As a result, the trace fits an exponential curve of the form

$$\Delta S(\tau)=S_0\left\{\exp\left[-\frac{\Gamma\Delta g_N^{\mathrm{sat}}L}{2T}\tau-\delta_T\right]-1\right\} \tag{4}$$

remarkably well [see the black thin line in Fig. 2(b)]. Here, S_0 is the probe pulse energy after propagating through the unperturbed SOA. $\Delta g_N^{\mathrm{sat}}$ is the initial steplike change in the local gain, uniform across the waveguide under full saturation conditions, due to carrier density depletion that later recovers as dictated by τ_N. The gain depletion due to carrier heating integrated along the length L_T is accounted for by the parameter δ_T. First, the validity of Eq. (4) was checked by fitting the trace calculated with the model for a pump pulse energy of $50E_{3\ \mathrm{dB}}$ [see the black thin line in Fig. 2(b)]. This fit gives $\Delta g_N^{\mathrm{sat}}=46\ \mathrm{cm}^{-1}$, in excellent agreement with the value of $45\pm1\ \mathrm{cm}^{-1}$ predicted by the model across the entire SOA. As shown in Fig. 2(a), the trace (III) measured at the highest pump pulse energy also fits to Eq. (4), yielding a value for $\Gamma\Delta g_N^{\mathrm{sat}}$ of $31.4\ \mathrm{cm}^{-1}$, and providing experimental

evidence of gain saturation along the entire length of the amplifier.

In Eq. (4), we have neglected the slow gain recovery and pulse width, since $\tau_N \gg 2T \gg \tau_p$. For delays smaller than a few picoseconds such that $\tau L/2T < L_T$, the probe travels across a perturbed portion of the SOA shorter than L_T. As a result, the total gain compression experienced by the probe due to carrier heating is smaller than δ_T and Eq. (4) is no longer valid (note how the fit diverges from the data of Fig. 2(b) for $\tau < 3$ ps).

Gain changes will be accompanied by changes in the refractive index, as expressed via the linewidth enhancement factors.[8] Therefore, larger negative slopes in the counter-propagating pump-probe traces shown in Fig. 2(a) translate into a sharper edge for the switching window of interferometric devices. Our results show that gain saturation across the entire device length would result in a narrower switching window than the length of the device would imply.

In this paper, counter-propagating pump-probe measurements with sub-picosecond pulses in a SOA are reported. These provide information on the spatial dependence of nonlinearities, namely, gain depletion and saturation, along the waveguide. In switching configurations with copropagating control and data pulses, only the control pulse duration dictates the sharpness of the switching window edge. However, counter-propagating schemes (e.g., TOAD or colliding pulse Mach–Zehnder) exhibit slow switch on/off, due to the device finite length. Although this limitation cannot be fully overcome, since the results in the counter-propagating geometry relate to the shape of the switching window in the above mentioned schemes, the measurements reported here demonstrate how systems could be optimized by adjusting parameters such as electrical bias and pump pulse energy. We show that the narrowest switching windows can be obtained in the limit when strong saturation is induced by the pump across the whole device length.

The authors are grateful to R. J. Manning for supplying the optical amplifier, and wish to thank the EPSRC and Nicol Trust for financial support.

[1] J. P. Sokoloff, P. R. Prucnal, I. Glesk, and M. Kane, IEEE Photonics Technol. Lett. **5**, 787 (1993).
[2] D. Cotter, R. J. Manning, K. J. Blow, A. D. Ellis, A. E. Kelly, D. Nesset, I. D. Phillips, A. J. Poustie, and D. C. Rogers, Science **286**, 1523 (1999).
[3] P. Toliver, T. Runser, I. Glesk, and P. R. Prucnal, Opt. Commun. **175**, 365 (2000).
[4] K. L. Hall, E. R. Thoen, and E. P. Ippen, *Semiconductors and Semimetals*, Vol. 59, Chap. 2 (Academic Press, 1999).
[5] M. Y. Hong, Y. H. Chang, A. Dienes, J. P. Heritage, P. J. Delfyett, S. Dijaili, and F. G. Patterson, IEEE J. Sel. Top. Quantum Electron. **2**, 523 (1996).
[6] R. P. Schreieck, M. H. Kwakernaak, H. Jäckel, and H. Melchior, IEEE J. Quantum Electron. **38**, 1053 (2002).
[7] G. Toptchiyski, S. Randel, K. Petermann, C. Schubert, J. Berger, and H. G. Weber, IEEE Photonics Technol. Lett. **14**, 534 (2002).
[8] C. H. Henry, IEEE J. Quantum Electron. **18**, 259 (1982).